Anal. Chem. **2001,** *73,* 4668−4675

A Portable, High-Speed, Vacuum-Outlet GC Vapor Analyzer Employing Air as Carrier Gas and Surface Acoustic Wave Detection

Joshua J. Whiting,[†] Chia-Jung Lu,[‡] Edward T. Zellers,[†,‡] and Richard D. Sacks*,[†]

Department of Chemistry and Department of Environmental Health Sciences, Center for Wireless Integrated Microsystems, University of Michigan, Ann Arbor, Michigan 48109

Vacuum-outlet GC with atmospheric-pressure air as the carrier gas is implemented at outlet pressures up to 0.8 atm using a low-dead-volume polymer-coated surface acoustic wave (SAW) detector. Increases in the system outlet pressure from 0.1 to 0.8 atm lead to proportional increases in detector sensitivity and significant increases in column efficiency. The latter effect arises from the fact that optimal carrier gas velocities are lower in air than in more conventional carrier gases such as helium or hydrogen due to the smaller binary diffusion coefficients of vapors in air. A 12-m-long, 0.25-mm-i.d. tandem column ensemble consisting of 4.5-m dimethyl polysiloxane and 7.5-m trifluoropropylmethyl polysiloxane operated at an outlet pressure of 0.5 atm provides up to 4 × 10^4 theoretical plates and a peak capacity of 65 (resolution, 1.5) for a 3-min isothermal analysis. At 30 °C, mixtures of vapors ranging in vapor pressure from 8.6 to 76 Torr are separated in this time frame. The SAW detector cell has an internal volume of <2 μL, which allows the use of higher column outlet pressures with minimal dead time. The sensor response is linear with solute mass over at least 2−3 decades and provides detection limits of 20−50 ng for the vapors tested. The combination of atmospheric-pressure air as carrier gas, modest operating pressures, and SAW sensor detection is well-suited for field instrumentation since it eliminates the need for support gases, permits smaller, low-power pumps to be used, and provides sensitivity to a wide range of vapor analytes.

The advantages of field-portable instrumentation for monitoring volatile and semivolatile organic compounds, relative to conventional sorbent tube or whole-air sampling methods followed by laboratory analysis, include the following: reduced sample handling, which minimizes loss, degradation, or contamination; greater sample throughput; and the potential for more timely responses to measurement results. Air samples containing more than a few organic components require separation by gas chromatography (GC) for accurate quantification of each component. Where nonspecific detectors are employed, qualitative analysis is based solely on retention time. Instruments employing GC with more sophisticated detectors, such as mass spectrometers or ion mobility spectrometers,[1−3] can provide more definitive identification of eluting species at the cost of increased size, power, complexity, and cost.

Early portable GC analyzers were limited by the relatively long times required for the separation of sample components. Reductions in separation times have been achieved by use of relatively short columns with high carrier gas flow rates,[4−6] microbore columns,[7,8] special inlets,[9,10] and fast temperature programming.[11,12] However, instruments capable of high-speed GC (HSGC) often have reduced resolution and sample capacity. Column temperatures are also limited in portable instruments due to power constraints, although improvements have been made by the use of efficient heater designs.[13,14] The need for inert carrier gas and, in the case of flame ionization detectors, hydrogen and air to support the flame can also be considered limitations of current field instruments.

In striving to simplify portable GC systems, Sacks et al. have recently explored the use of vacuum-outlet HSGC with atmospheric-pressure air as carrier gas.[15−18] Although the high viscosity of air, relative to H_2 or He carrier gases, leads to a more rapid loss in column efficiency at higher flow rates, this is partially offset by operating at subambient pressure. Furthermore, reductions in detector dead time are achieved under such conditions because of increases in carrier gas velocities through the detector cell.[17]

[†] Department of Chemistry.
[‡] Department of Environmental Health Sciences.

(1) Piltingsrud, H. *Am. Indust. Hyg. Assoc. J.* **1997**, *58*, 564.
(2) *Hapsite by Inficon*, URL http://www.hapsite.com/.
(3) *Femtoscan*, URL http://www.femtoscan.com/.
(4) Cramers, C.; Scherenzeel, G.; Leclercq, P. *J. Chromatogr.* **1981**, *203*, 207.
(5) Jonker, R.; Poppe, H.; Huber, J. *Anal. Chem.* **1982**, *54*, 2447.
(6) Simon, J.; Szepesy, L. *J. Chromatogr.* **1976**, *119*, 495.
(7) Van Es, A. *High-Speed Narrow Bore Capillary Gas Chromatography;* Huthig Buch Verlag: Heidelberg, Germany, 1992.
(8) Van Es, A.; Janssen, J.; Bally, R.; Cramers, C.; Rijks, J. *J. High. Resolut. Chromatogr.* **1987**, *10*, 273.
(9) Klemp, M.; Peters, A.; Sacks, R. *Environ. Sci. Technol.* **1994**, *28*, 369 A.
(10) Ehrmann, E. U.; Dharmasema, H. P.; Carney, K.; Overton, E. B. *J. Chromatogr. Sci.* **1996**, *34*, 533.
(11) Grall, A.; Leonard, C.; Sacks, R. *Anal. Chem.* **2000**, *72*, 591.
(12) Leonard, C.; Grall, A.; Sacks, R. *Anal. Chem.* **1999**, *71*, 2123.
(13) Overton, E. B.; Carney, K. R.; Dahrmasena, H. P.; Ashton, B. M.; Roques, N. J. *Abstr. Pap. Am. Chem. Soc.* **1998**, *216*, 1
(14) RVM Scientific, Inc., 600 Ward Drive, Ste. C-2, Santa Barbara, CA 93111.
(15) Smith, H.; Zellers, T.; Sacks, R. *Anal. Chem.* **1999**, *71*, 1610.
(16) Grall, A.; Sacks, R. *Anal. Chem.* **1999**, *71*, 5199.
(17) Grall, A.; Sacks, R. *Anal. Chem.* **2000**, *72*, 2507.
(18) Grall, A. J.; Zellers, E. T.; Sacks, R. D. *Environ. Sci. Technol.* **2001**, *35*, 163.

10.1021/ac0103726 CCC: $20.00
Published on Web 09/05/2001

Stationary-phase materials capable of withstanding prolonged exposure to air at elevated temperatures without degradation have also been identified.[16]

These initial studies of vacuum-outlet HSGC with atmospheric-pressure air as carrier gas used a photoionization detector (PID). Although this type of detector is well-suited for vacuum-outlet GC, commercial PIDs have relatively large cell volumes (~100 μL), which requires column outlet pressures of <0.1 atm to reduce detector band broadening to acceptable levels.[15−18] Since such low pressures are not easily achieved with pumps suitable for field instrumentation, operation at higher (subambient) pressures must be considered, which, in turn, requires a low-dead-volume detector. If operation without support gases is to be achieved, flame-based detectors are precluded. In addition, these detectors are not designed to function at subambient outlet pressure. Thermal conductivity detection (TCD) with air as carrier gas is not feasible due to the similarity in the thermal conductivity of air and that of most organic vapors.

Microfabricated chemical sensors present an intriguing alternative to conventional GC detectors for this application. Among the microsensor technologies that have been developed in recent years, those based on acoustic wave devices have a number of attractive features. Included in this class of sensors are the thickness shear mode (TSM) (also known as quartz crystal microbalance), flexural plate wave, and surface acoustic wave (SAW) sensors.[19−23] When coated with sorptive polymers, these sensors provide rapid, reversible responses to most vapors and linear response isotherms over fairly large ranges of concentration.[24,25] Operation at low temperatures is also an advantage.

Use of polymer-coated TSM sensors as GC detectors was reported in some of the earliest work on these chemical sensors[26−28] and has been revisited recently.[29,30] In addition, SAW sensors have been used as GC detectors, with[31−33] and without[34,35] polymer coatings. Recent reports by Frye-Mason et al.[33,36−38] describe the development of a microanalytical system employing an integrated array of four polymer-coated SAW sensors coupled to upstream preconcentrator and etched-channel GC separation modules and a downstream sampling pump. This system is designed to determine low concentrations of warfare agent simulants, and preliminary results are encouraging.

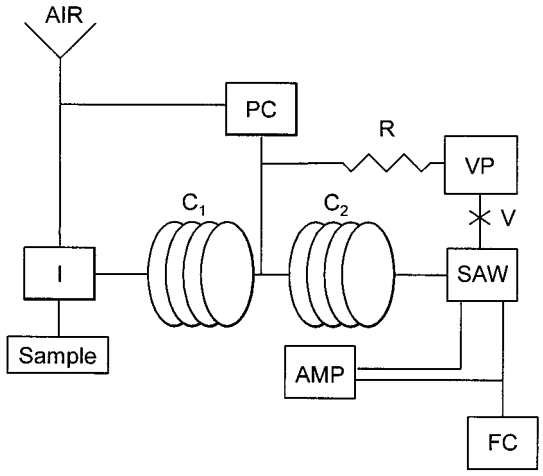

Figure 1. Experimental platform: I, cryofocusing inlet system; C_1 and C_2, nonpolar and polar columns; SAW, surface acoustic wave detector; AMP, feedback amplifier; FC, frequency counter; VP, vacuum pump; PC, pressure controller; V, valve; R, capillary pneumatic restrictor.

Integrated SAW sensor arrays have two very important features for vacuum-outlet HSGC of complex mixtures of airborne organic vapors. First, the patterns of responses from the array can be used together with retention times to enhance the ability to identify both fully resolved and coeluting mixture components.[18,32,39] Thus, the burden of selectivity can be shared between the column and the detector. Second, these small arrays can be packaged in very low volume cells, which make it feasible to consider vacuum-outlet column operation at higher outlet pressures where smaller, lighter weight vacuum pumps can be used.

None of the studies employing acoustic wave sensors as GC detectors has explored the implications of using vacuum-outlet HSGC with atmospheric-pressure air as carrier gas in terms of chromatographic efficiency or detector response. The work reported here considers this topic using polymer-coated SAW sensor detection, with specific focus on the effect on column holdup time, column resolving power, analysis time, and detector response characteristics of using outlet pressures ranging from 0.1 to 0.8 atm.

EXPERIMENTAL SECTION

Apparatus. The schematic diagram in Figure 1 shows the vacuum-outlet GC configuration used to evaluate the SAW sensor

(19) Hierlemann, A.; Ricco A. J.; Bodenhöfer K.; Dominik, A.; Göpel, W. *Anal. Chem.* **2000**, *72*, 3696.
(20) Cai, Q. Y., Park, J., Heldsinger, D., Hsieh, M. D., and Zellers, E. T. *Sens. Actuators, B* **2000**, *62*, 121.
(21) Park, J.; Groves, W. A.; Zellers, E. T. *Anal. Chem.* **1999**, *71*, 3877.
(22) Martin, S. J.; Frye, G. C.; Senturia, S. D. *Anal. Chem.* **1994**, *66*, 2201.
(23) Hierlemann, A.; Zellers, E. T.; Ricco, A. J. *Anal. Chem.* **2001**, *73*, 3458−3466.
(24) Ballantine, D. S.; White, R. M.; Martin, S. J.; Ricco, A. J.; Zellers, E. T.; Frye, G.; Wohltjen, H. *Acoustic Wave Sensors: Theory, Design, and Physicochemical Applications;* Academic Press: Boston, MA, 1997.
(25) Grate, J. W. *Chem. Rev.* **2000**, *100*, 2627.
(26) King, W. H. *Anal. Chem.*, **1964**, *36*, 1735.
(27) Janghorbani, M.; Freund, H. *Anal. Chem.* **1973**, *45*, 325.
(28) Karasek, F. W.; Guy, P.; Hill, H. H.; Tiernay, J. M. *J. Chromatogr.* **1976**, *124*, 179.
(29) Chang, P.; Shih, J.-S. *Anal. Chim. Acta* **1999**, *380*, 55−62.
(30) Rocha-Santos, T. A. P; Gomes, M. T. S. R.; Duarte, A. C.; Oliveira, J. A. B. P. *J. Environ. Monit.* **2000**, *2*, 277.
(31) Hofmann, T.; Schieberle, P.; Krummel, C.; Freiling, A.; Bock, J.; Heinert, L.; Kohl, D. *Sens. Actuators, B* **1997**, *41*, 81.
(32) Lu, C. J. and Zellers, E. T. *Anal. Chem.* **2001**, *73*, 3449−3457.
(33) Manginell, R. P.; Frye-Mason, G. C.; Lewis, P. R.; Kottenstette, R. J.; Heller, E. J.; Adkins, D. R.; Dulleck, G. R.; Martinez, D.; Mowry, C. D.; Anderson, L. F. *198th Meeting of the Electrochemical Society, Meeting Abstracts*; Phoenix, AZ, October 22−27, 2000; ECS, Inc.: Pennington, NJ, 2000; Abstract 1094.
(34) *znose*, URL http://www.estcal.com
(35) Williams, D.; Pappas, G. *Field Anal. Chem. Technol.* **1998**, *2* (5), 299.
(36) Frye-Mason, G.; Kottenstette, R.; Lewis, P.; Heller, E.; Manginell, R.; Adkins, D.; Dulleck, G.; Martinez, D.; Sasaki, D.; Mowry, C.; Matzke, C.; Anderson, L. *Proc. Micro Total Analysis Systems 2000*; Kluwer Academic Publishers: Boston, MA, 2000; pp 229−232.
(37) Heller, E. J.; Hietala, V. M.; Kottenstette, R. J.; Manginell, R. P.; Matzke, C. M.; Lewis, P. R.; Casalnuovo, S. A.; Frye-Mason, G. C. In *Proc. Electrochemical Society*; Butler, M., Yamazoe, N., Vanysek, P., Aizawa, M., Eds.; ECS, Inc.: Pennington, NJ, 1999; Vol. 99-23, pp 138−142.
(38) Frye, G. C.; Cernosek, R. W.; Martin, S. J.; Pfeifer, K. B.; Gilbert, D. W. Extended Abstracts, Electrochemical Society Meeting, Miami Beach, FL, Oct 9−14, 1994; ECS, Inc.: Pennington, NJ, 1994; Abstract 665, pp 1046−1047.
(39) Park, J.; Groves, W. A.; Zellers, E. T. *Anal. Chem.* **1999**, *71*, 3877.

array and the effects of column outlet pressure. A cryofocusing inlet system I (model L Cryointegrator, Chromatofast, Inc., Ann Arbor, MI) provides a sample injection plug width of ~10 ms.[40] While this inlet device is not suitable for a portable instrument, it is useful for reducing inlet band broadening, which simplifies studies of the effects of outlet pressure on column efficiency and detector performance. The inlet uses a metal capillary tube cooled to ~−80 °C to collect and focus organic vapor samples from an atmospheric-pressure gas-sampling bag or bottle. A small, on-board vacuum pump pulls the sample through the tube at a rate of ~1 cm^3/min. Software-adjustable sample collection time is used to control the amount of sample collected in the tube. The tube is then rapidly heated to ~250 °C by the current surge from a capacitive-discharge power supply, and the resulting vapor is injected into the column.[41]

Tank air, purified to remove water vapor and hydrocarbons, is supplied to the inlet system, and a pressure gauge located between the inlet system and the column is used to set the column head pressure to an absolute pressure of 1.0 atm. A portable instrument utilizing this technology will use scrubbers to remove water vapor and organic compounds from ambient air, and pressure drops along these devices will result in a column head pressure less than ambient pressure.

The series-coupled column ensemble, C_1 and C_2, consists of a 4.5-m length of nonpolar dimethyl polysiloxane (DB-1, J&W Scientific, Folsom, CA) for the first column followed by a 7.5-m length of trifluoropropylmethyl polysiloxane (Rtx-200, Restek, Bellafonte, PA). Both columns have 0.25-mm i.d. and use 0.25-μm-thick bonded stationary phases. An electronic pressure controller PC (with pneumatic restrictor R) can be used to control the carrier gas (air) pressure at the column junction point in order to tune the selectivity of the column ensemble for specified sets of target compounds.[42,43] This feature was not used in the present study, and the column ensemble was operated with a junction pressure set point equal to the pressure that would occur in the absence of any other external connections. These set-point pressure values were calculated for various ensemble outlet pressures from standard equations for gas flow in capillary tubes.[15,17] This procedure keeps the ratio of holdup times for the two columns nearly constant and is necessary so that the outlet pressure could be varied over a relatively wide range without large changes in ensemble selectivity. Vacuum pump VP (UN84.3 ANI, KNF Neuberger, Inc., Trenton, NJ) is used to drive the separation. Valve V (55-4 μ_BG, Nupro Co., Willoughby, OH) is used to set the detector pressure. A pressure gauge (px304-050AV, Omega Engineering, Inc., Stamford, CT, not shown in the figure) is located between the detector and the valve.

The cryofocusing inlet device and the junction-point pressure controller are interfaced to a PC with a 16-bit A/D board (CIODAS 1602, Computer Boards, Inc., Mansfield MA). Data acquisition and instrument control functions are implemented with LABTECH notebook software (Laboratory Technologies, Inc., Wilmington, VA). Chromatograms were processed with Grams/32 v. 4.04 software (Galactic Industries, Salem, NH)

Table 1. Compounds Used in Test Mixtures

no.	compound	bp (°C)	k_o[a]
1	ethyl acetate	77	1.0
2	benzene	80	0.9
3	trichloroethylene	87	1.2
4	2,4-dimethylhexane	109	1.5
5	toluene	111	2.4
6	tetrachloroethylene	121	3.1
7	octane	126	2.7
8	butyl acetate	126	6.0
9	chlorobenzene	130	5.1
10	ethylbenzene	136	5.6
11	*p*-xylene	138	6.1

[a] Values at 30 °C.

SAW Sensor Array. The detector consists of an array of four ST-quartz SAW delay lines sealed beneath a Pyrex lid having inlet and outlet ports fitted with passivated fused-silica capillaries. The detector was designed and constructed by researchers at Sandia National Laboratories and graciously provided to us for this study. A large central launching transducer generates acoustic waves that are received by each of four smaller transducers, two on each side of the central transducer. Each sensor has an active sensing area of ~0.3 mm^2, and the entire cell occupies an area of ~6 mm^2. The detector dead volume is ~2 μL. Details of detector design and operation can be found elsewhere.[38] The nominal operating frequency of each sensor is 389 MHz. For the testing performed in this study, only one of the four sensors in the array was monitored. This sensor was spray-coated with polyisobutylene (PIB) to a frequency shift of 1.1 MHz, corresponding to a coating thickness of ~65 nm.

The sensor was placed in a feedback loop with a dual-stage wide-band amplifier (B447D.001, Hewlett-Packard, Palo Alto, CA), and the output frequency was measured with a frequency counter (model 53131A, Hewlett-Packard) and logged via an HPIB interface by a personal computer. Output signals were acquired at a rate of 18 Hz using Benchlink Meter software (version 1.0, Hewlett-Packard).

The sensor array was located outside the GC oven and was operated at ambient temperature. A 10-cm-long segment of 0.25-mm-i.d. deactivated fused-silica tubing was used to connect the end of the column ensemble to a capillary fitting provided with the sensor array. Typically, these sensors show a 4−5% decrease in response for a 1 °C increase in temperature.[44]

Materials and Procedures. Table 1 lists the compounds used to prepare vapor test mixtures. Ensemble retention factors at 30 °C also are listed. Samples were prepared by injecting 5 μL of each component into a 4-L glass sampling bottle and diluting with dry nitrogen. Quantitative evaporation occurs for all components in the test mixture. The capillary inlet tube from the cryofocusing device was inserted through a septum in the sample bottle cap. Sample collection in the cryofocusing device is quantitative for the conditions used here, and the injected sample mass is proportional to the product of the software-selectable sample collection time and the sample vapor concentration in the bottle.[41] All separations used an oven temperature of 30 °C.

(40) Klemp, M; Peters, A; Sacks, R. *Environ. Sci. Technol.* **1994**, *28*, 369A.
(41) Akard, M.; Sacks, R. D. *J. Chromatogr. Sci.* **1994**, *32*, 499.
(42) Leonard, C.; Sacks R. D. *Anal. Chem.* **1999**, *71*, 5501.
(43) Sacks, R.; Coutant, C.; Veriotti, T.; Grall, A. *J. High Resolut. Chromatogr.* **2000**, *23*, 225.
(44) Zellers, E. T.; Han M. *Anal. Chem.* **1996**, *68*, 2409.

RESULTS AND DISCUSSION

Vacuum-Outlet GC. Important parameters that are dependent on outlet pressure include volumetric flow rate, column holdup time, column efficiency, detector response time, and detector sensitivity. Since inlet pressure cannot be adjusted, any change in column length or outlet pressure inevitably results in changes in volumetric flow rate, average carrier gas velocity, and column holdup time.

The required pumping speed can be found from the column outlet pressure p_o and the volumetric flow rate F of carrier gas (air). Volumetric flow rate at the inlet pressure of 1.0 atm is given by eq 1, where r is the internal column radius, η is the carrier

$$F = \pi r^4 (1 - p_o^2)/16\eta L \qquad (1)$$

gas viscosity, L is the column length, and the outlet pressure is expressed in atmospheres. For $p_o = 1.0$ atm, $F = 0$, and for $p_o \ll 1$ atm, F is nearly independent of p_o.

The average linear carrier gas velocity u is important in determining the column efficiency and thus the resolving power of any specified column length. The value of u is given by eq 2.

$$u = \frac{3r^2(1 - p_o^2)^2}{32\eta L(1 - p_o^3)} \qquad (2)$$

For $p_o = 1.0$ atm, $u = 0$, and for $p_o \ll 1$ atm, u is independent of p_o.

Panels a and b of Figure 2 show plots of volumetric flow rate and average linear carrier gas velocity, respectively, versus p_o under standard conditions (0 °C and 1.0 atm) for 0.25-mm-i.d. columns with length indicated by each plot. The volumetric flow rate is expressed as standard cm^3/min (sccm). The decrease in F with increasing column length is clearly seen. The effects of p_o are relatively small for the lower p_o values, but as p_o approaches 1 atm, F decreases more rapidly with increasing p_o. The column ensemble used for this study is 12 m long, and F is 1.1 sccm at 0.5-atm outlet pressure.

The optimal average carrier gas velocity u_{opt} (velocity giving the minimum height equivalent to a theoretical plate) for an open-tubular column is found by differentiation of the Golay equation for column efficiency.[45] Equation 3 gives the expression for u_{opt}

$$u_{opt} = \frac{3D_g p_o(1 - p_o^2)}{2r(1 - p_o^3)} \sqrt{\frac{48(k+1)^2}{1 + 6k + 11k^2}} \qquad (3)$$

for the case of 1-atm inlet pressure and a thin-film column where resistance to mass transport in the stationary phase can be neglected and where k is the retention factor of a given analyte at the column temperature and D_g is the binary diffusion coefficient of the analyte in the carrier gas at the column outlet pressure.

The dashed lines in Figure 2b show u_{opt} assuming an atmospheric-pressure D_g value of 0.08 cm^2/s. This is close to the value for benzene in air at 30 °C.[46] Values of D_g at the column outlet pressure are found by dividing the atmospheric-pressure values of D_g by p_o.[46] The upper dashed line plot is for a k value of 0.1, and the lower dashed line plot is for a k value of 5.0. This spans the range of k values that are most frequently encountered for isothermal HSGC. Note that the u_{opt} values show only a weak dependence on the outlet pressure. This has been discussed[16] and is the result of constraining the inlet pressure to 1.0 atm.

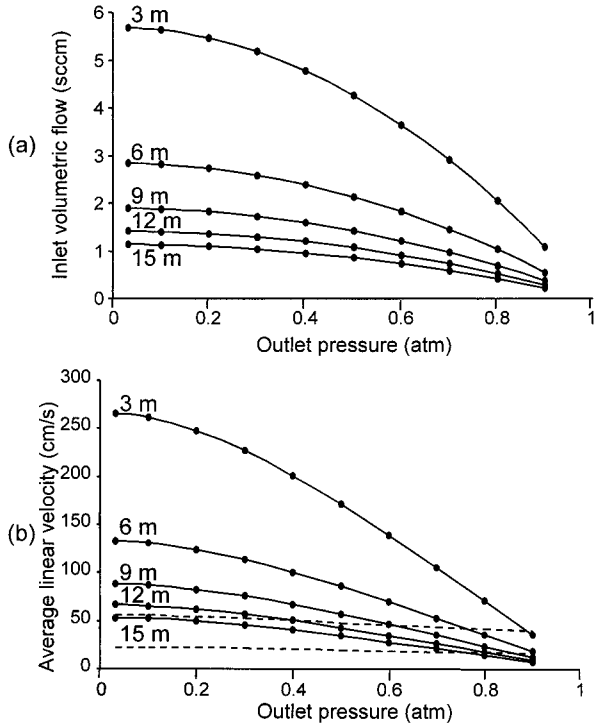

Figure 2. Volumetric flow rate (a) and average carrier gas velocity (b) vs outlet pressure for a 0.25-mm-i.d. column using air as carrier gas at an inlet pressure of 1.0 atm and column length as indicated by each plot.

The values of u_{opt} plotted in Figure 2b are significantly lower than for hydrogen or helium carrier gas because of the smaller values of D_g in air. This presents a significant limitation to the use of air as a carrier gas for HSGC. In addition, the increase in the height equivalent to a theoretical plate for u values significantly greater than u_{opt} is greater with air than with the other carrier gases.[16] For these reasons, it is desirable to operate near u_{opt}. From Figure 2b, it is clear that the u values for the shortest column are too high for efficient column operation except for outlet pressures near 1 atm. For the 12-m-long column ensemble used in this study, u values are in the range of the u_{opt} values for p_o from 0.4 to 0.8 atm, depending on the values of retention factor.

Under isothermal conditions, retention time t_R for any mixture component is given by eq 4, where t_m is the column holdup time.

$$t_R = t_m(k + 1) \qquad (4)$$

For a 1-atm inlet pressure, holdup time is given by eq 5. For $p_o \ll 1$ atm, t_m is nearly independent of p_o but increases with the square of the column length. For the higher outlet pressures used in this work, t_m increases rapidly with increasing outlet pressure.

(45) Ingraham, D.; Shoemaker, C.; Jennings, W. *HRC & CC, J. High Resolut. Chromatogr. Chromatogr. Commun.* **1981**, *5*, 227.

(46) Fuller, E. N.; Schettler, P. D.; Giddings, J. C. *Ind. Eng. Chem.* **1966**, *58*, 19.

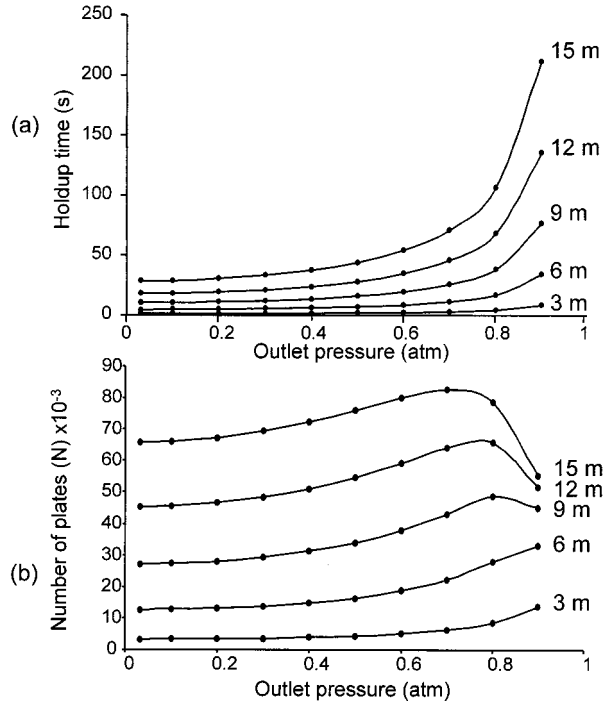

Figure 3. Holdup time (a) and number of theoretical plates (b) vs outlet pressure for a 0.25-mm-i.d. column using air as carrier gas at an inlet pressure of 1.0 atm and column length as indicated by each plot. For plots b, a retention factor of 2.0 and a binary gas-phase diffusion coefficient of 0.08 cm^2/s were assumed. Band broadening from nonequilibrium effects in the stationary phase and from extra-column sources were neglected.

$$t_m = \frac{32\eta L^2(1 - p_o^3)}{3r^2(1 - p_o^2)^2} \quad (5)$$

Figure 3a shows plots of t_m versus p_o for the case of 1-atm air at the inlet at a temperature of 30 °C. Plots are shown for the same lengths of 0.25-mm-i.d. column as in Figure 2. As expected, for p_o less than ~0.4 atm, t_m shows only a weak dependence on p_o. For higher p_o, *tm* and thus the isothermal analysis time increases more rapidly with increasing p_o, particularly for the longer columns. For HSGC, a typical isothermal analysis may span a *k* range from 0 to 5. If the analysis time is to be kept less than 3 min, for example, then from eq 4, t_m should be no larger than ~30 s. For the 12-m-long column used in the present study, a holdup time of 30 s or less can be achieved with a p_o value of 0.5 atm or less.

The Golay equation for column efficiency[47] together with the column length was used to compute the number of theoretical plates as a function of outlet pressure for atmospheric-pressure air as carrier gas at 30 °C. A retention factor of 2 and a gas-phase binary diffusion coefficient of 0.08 cm^2/s at atmospheric pressure were assumed. Results are shown in Figure 3b for the same lengths of 0.25-mm-i.d. column as in Figure 2. Note that band broadening in the stationary phase and from extracolumn sources was neglected. Previous work[16] has shown that neglecting stationary-phase band broadening is valid for the 0.25-μm-thick dimethyl polysiloxane and trifluoropropylmethyl polysiloxane stationary phases used in the present system.

(47) Golay, M. In *Gas Chromatography 1958*; Desty, D., Ed.; Academic Press: New York, 1958; p 36.

For lower p_o, *u* is greater than u_{opt} for all but the longest column, and the number of plates produced by the columns is relatively low. As p_o increases, *u* decreases, and the columns become more efficient. For an outlet pressure in the range 0.7–0.8 atm, the longer columns show maximum plate production. For still higher p_o, *u* is less than u_{opt} for the longer columns, and column efficiency decreases due to increased band broadening from longitudinal diffusion. For the shorter columns, the *u* values are greater, and the maximum number of plates occurs at higher p_o. For the 3-m-long column, even for p_o as large as 0.9 atm, *u* is greater than u_{opt}. The results from Figures 2 and 3 indicate that, for the case of atmospheric-pressure air as carrier gas and a 12-m column length, p_o in the range 0.4 0.7 atm represents a reasonable compromise between analysis time and column resolving power.

System Performance. Figure 4 shows chromatograms obtained with atmospheric-pressure air as carrier gas and the SAW detector. The numbers to the left of the chromatograms indicate the column outlet pressure in atmospheres. The peak numbers correspond to the compound numbers in Table 1. The large peak at the beginning of each chromatogram is from water vapor, which is collected in the cryofocusing inlet system and injected along with the organic mixture components. For these test chromatograms, between 90 and 200 ng of each component was injected.

As the outlet pressure increases from top to bottom in Figure 4, the analysis time increases slowly at first and then rapidly as the outlet pressure approaches 1 atm. This is consistent with the plots shown in Figure 3a. For the 0.5-atm case, the analysis is complete in ~200 s. While the use of outlet pressures as high as 0.8 atm is attractive in reducing vacuum pump requirements, the more than 2-fold increase in analysis time relative to an outlet pressure of 0.5 atm must be considered.

As the column outlet pressure increases, the signal produced by the SAW sensor also increases. This is discussed in the following section. Also note the elution order change that occurs for components 8 (butyl acetate) and 11 (*p*-xylene) as the column outlet pressure is changed. This is an artifact of the pressure-tunable column ensemble used in this study.

Figure 5 shows plots of the number of theoretical plates measured for four of the peaks in Figure 4. Components 8 and 11 were omitted because they coeluted over a considerable range of outlet pressures. The number of plates *N* was calculated using eq 6, where $W_{1/2}$ is the full peak width at half-height. Differences

$$N = 5.545(t_R / W_{1/2})^2 \quad (6)$$

in the gas-phase diffusion coefficients and retention factors for the different solutes are partly responsible for the range of values observed for the different compounds for any specified outlet pressure. Solute-specific band broadening in the detector also cannot be ruled out.

The general increase in the number of plates as the outlet pressure is increased is consistent with expectations from Figure 3b. The more rapid increase as the outlet pressure approaches 1 atm is consistent with predictions. The number of plates generated by the column ensemble also is in reasonable agreement with the values from Figure 3b, particularly at higher outlet pressures. Note that the plate number values in Figure 3b are for specified

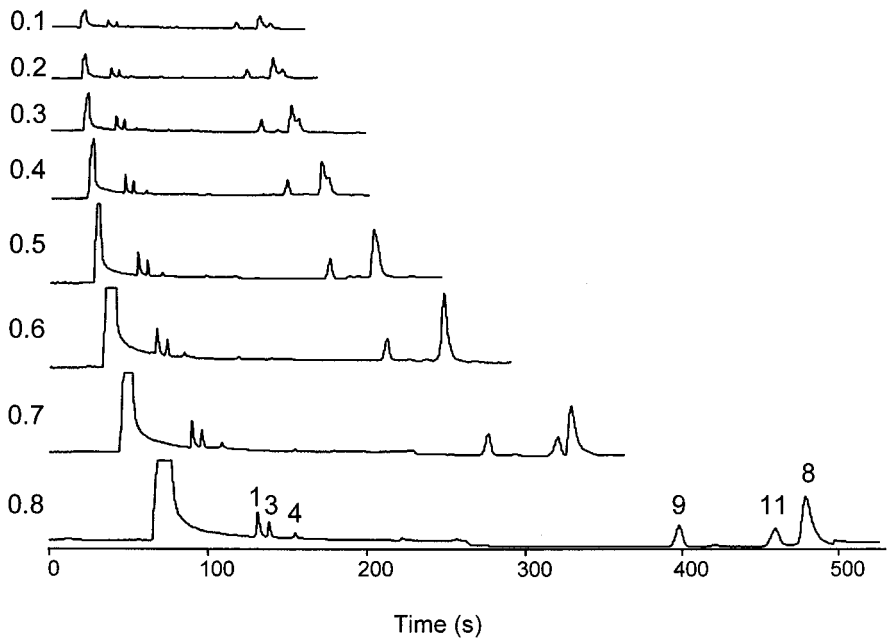

Figure 4. Chromatograms of a test mixture with the outlet pressures (atm) given to the left of each chromatogram. Peaks labels correspond to component numbers in Table 1. Air was used as carrier gas with an absolute inlet pressure of 1.0 atm.

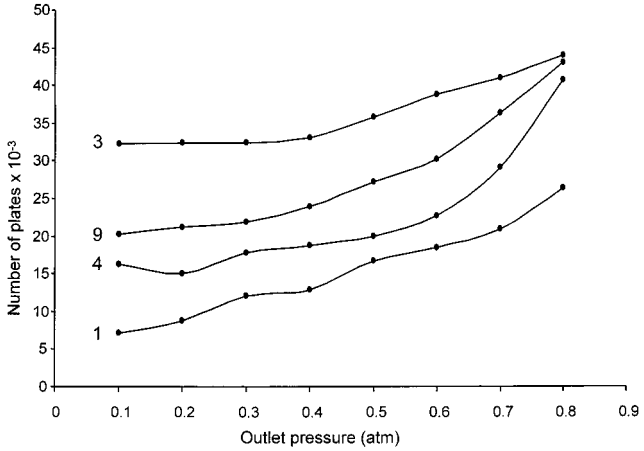

Figure 5. Number of theoretical plates from eq 6 vs outlet pressure for components 1, 3, 4, and 9 from Table 1. Air was used as carrier gas with an absolute inlet pressure of 1.0 atm.

values of k and D_g, and consider only longitudinal diffusion and nonequilibrium effects in the gas phase.

A significant limitation of using relativity high outlet pressure is the increased analysis time. In some applications this may be acceptable, and the ability to obtain high-quality chromatograms using atmospheric-pressure air as carrier gas with an outlet pressure as modest as 0.8 atm is noteworthy. A significant advantage in operation at the higher outlet pressures is the increase in resolving power due to the lower (more nearly optimal) average carrier gas velocities. It is also clear from Figure 4 that the detector response is greater at higher outlet pressure.

SAW Sensor Detection for HSGC. The SAW sensor is a mass-sensitive device. The analyte mass sorbed by the polymer coating depends on the gas-phase analyte concentration (equilibrium response) and possible nonequilibrium effects caused by limited rates of mass transport in both the gas and polymer phases. Detector band broadening depends on instrumental dead time resulting from the finite internal volume of the detector cell and possible band broadening from nonequilibrium effects in the gas and polymer phases.

Analyte concentration in the detector cell varies inversely with the volume of carrier gas in which the analyte elutes. For the case of 1-atm inlet pressure, the volumetric flow rate at the column outlet pressure F_o is given by eq 7. At low p_o, F_o decreases linearly

$$F_o = \frac{\pi r^4 (1 - p_o^2)}{16 p_o \eta L} \tag{7}$$

with increasing p_o, and thus, detector response should increase linearly with increasing p_o. At higher p_o values, gas compression effects result in a nonlinear decrease in F_o with increasing p_o.

An important feature of the SAW sensor array used in this work is low internal volume (estimated at 2 μL). This reduces detector dead time and allows the use of higher outlet pressures. Detector dead time (analyte residence time) can be estimated as the ratio of the detector cell volume to F_o. For a p_o value of 0.5 atm, F_o is ~2 cm^3/min and the dead time is ~0.06 s. This accounts for less than 1% of the variance of a 1-s-wide peak and can be neglected. These calculations assume plug flow through the detector and may underestimate detector dead time.

Nonequilibrium effects in the detector can be estimated from the diffusion path lengths in the gas and polymer phases and the corresponding diffusion coefficients. In the gas phase, the average diffusion path length x is half the distance from the polymer surface to the opposite cell wall. From the sensor array volume and surface area (~6 mm^2), x is found to be ~0.16 mm. For benzene in air at a pressure of 0.5 atm, D_g is ~0.16 cm^2/s, and the rms diffusion time t is found from the Einstein equation for one-dimensional diffusion.

$$t = x^2/2D_g \tag{8}$$

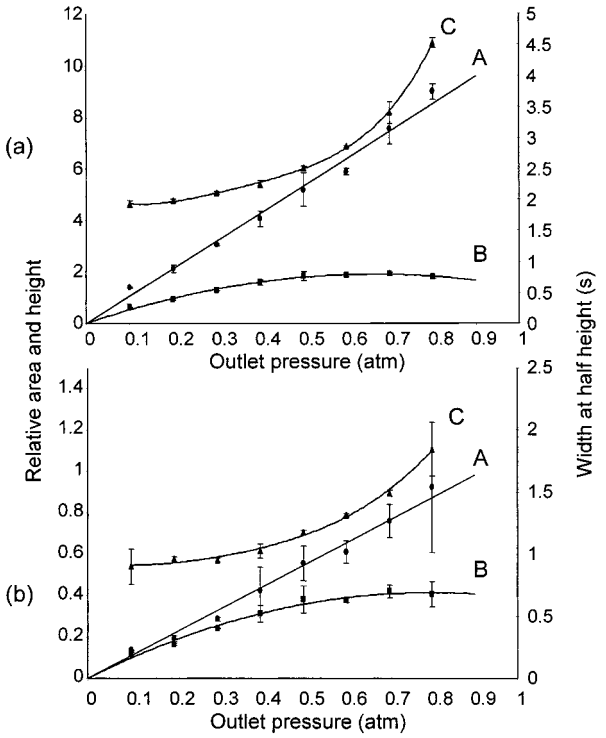

Figure 6. Peak area A, peak height B, and peak width C vs outlet pressure for components 4 (a) and 9 (b) from Table 1 using the SAW detector. Air was used as carrier gas with an absolute inlet pressure of 1.0 atm.

This gives an rms diffusion time in the gas phase of 0.0008 s. Since this is small compared to the 0.06-s analyte residence time, gas-phase nonequilibrium effects should be insignificant. The polymer coating used in the sensor is ~0.065 μm thick, and by analogy with stationary-phase film thickness values used in wall-coated capillary columns, analyte diffusion times should be small relative to the 0.06-s residence time.

Figure 6 shows plots of peak area (A), peak height (B), and peak width (C) versus column outlet pressure for 2,4-dimethylhexane (a) and chlorobenzene (b). Injected masses were 170 and 210 ng, respectively. Error bars show standard deviations for three replicate injections. These data were collected over a period of several days, and ±1−2 °C fluctuations in room temperature were typical. A linear increase in peak area with increasing p_o is observed for both solutes over the indicated pressure range.

For low p_o values, peak widths are relatively independent of p_o. For larger p_o values, peak widths increase significantly with increasing p_o. These trends are the result of rapidly increasing retention times and slowly increasing plate number with increasing p_o for the higher outlet pressure values. Peak height increases with increasing outlet pressure for pressures up to ~0.5 atm. For higher outlet pressures, peak height becomes more or less independent of pressure. This is the result of the increase in peak width with increasing pressure for larger p_o. Similar results were obtained for other components in the test mixture.

Detector reproducibility was evaluated for replicate injections made over a period of ~15 min using the same sample and the same sample collection time. Figure 7 show typical results for three replicate chromatograms. Peak numbers correspond to the component numbers in Table 1. The sample size for each chromatogram was 90−200 ng of each component. Peak area relative standard deviations are typically in the ±1−2% range.

Figure 8 shows analytical curves (log peak area vs log analyte mass) for several components in the test mixture. Numbers near the plots correspond to the mixture component numbers in Table 1. Sample concentrations in the gas sampling bottle and sample collection time in the cryofocusing inlet device were both varied to span the indicated concentration range. These data were collected over several days, and a significant portion of the point scatter can be attributed to fluctuations in the room temperature. The straight lines are from linear regression fits to the log−log data.

Table 2 summarizes data from the analytical curves in Figure 8. The log−log slopes are all within the range 1.05−1.1. This indicates reasonably good linearity of peak area with sample mass.

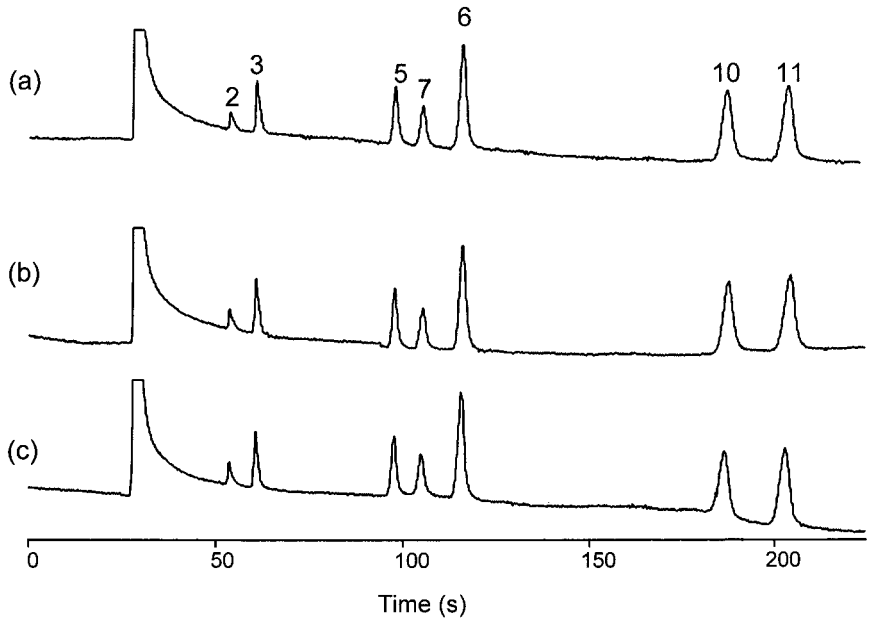

Figure 7. Three replicate chromatograms obtained with the SAW detector using the experimental platform shown in Figure 1 and atmospheric-pressure air as carrier gas The outlet pressure was 0.5 atm.

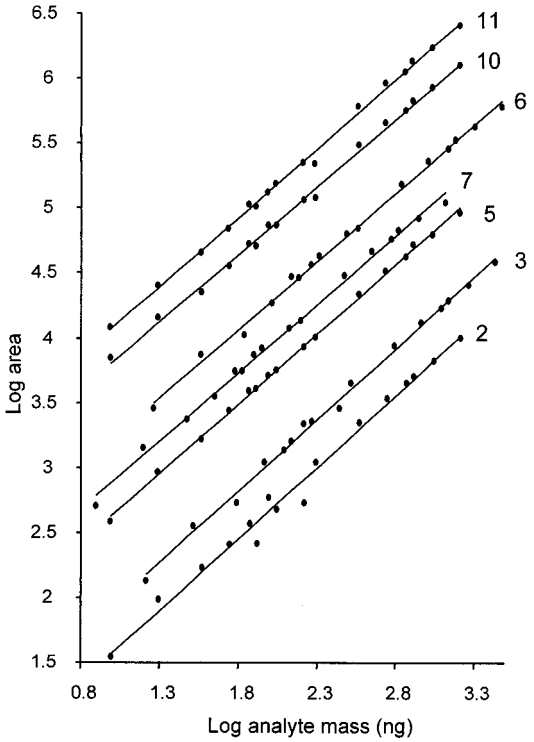

Figure 8. Log peak area vs log analyte mass for some of the mixture components listed in Table 1 using the SAW detector. Numbers near plots correspond to the component numbers in Table 1. See text for details.

Table 2. Summary of Analytical Results for Figure 8

no.	compound	slope	R^2	LOD (ng)
2	benzene	1.0993	0.9883	46
3	octane	1.0950	0.9965	47
5	tetrachloroethylene	1.0706	0.9988	35
6	ethylbenzene	1.0497	0.9962	23
7	trichloroethylene	1.0449	0.9969	24
10	toluene	1.0338	0.9971	30
11	*p*-xylene	1.0577	0.9973	33

With the exception of benzene, the correlation coefficients for the regression fits are all greater than 0.996. Limits of detection were computed for a signal-to-noise ratio of 3. Peak area noise was measured in an open region of the chromatogram adjacent to the peaks. Values range from 23 ng for ethylbenzene to 47 ng for *n*-octane.

CONCLUSIONS

This initial study has illustrated several of the operational tradeoffs, as well as establishing the feasibility, of gas chromatographic instrumentation employing subambient pressure air as carrier gas and polymer-coated SAW sensor detection. As shown here, optimal linear velocities can be achieved for modest column lengths (~9−12 m) at pressures in the range of 0.5−0.8 atm, which are within the operating range of many miniature low-power vacuum pumps. Total theoretical plate counts under these operating conditions are reasonably high. The tradeoff between isothermal analysis times and chromatographic resolution was also illustrated, and with temperature programming, analysis times could be reduced significantly with minimal loss of resolution. Additional work is needed to show feasibility for field measurements where ambient temperature, pressure, and moisture content are variable.

The polymer-coated SAW sensor is quite useful for portable HSGC instrumentation. Detector band broadening did not appear to be important for the conditions used in this study, owing in large measure to the small detector dead volume and also to rapid analyte sorption/desorption in the thin polymeric sensor layer. Increases in outlet pressure lead to proportional increases in sensor responses, as expected from thermodynamic considerations, which favors the use of higher outlet pressures. For the subambient pressure ranges considered, SAW sensor sensitivity is reduced by up to a factor of 2 relative to ambient-pressure operation.

A prototype instrument with components similar to those described here has been constructed. It employs a thermally desorbed adsorbent-based preconcentrator to collect organic vapors from 1-L air samples, which permits detection limits with the SAW sensor in the low part-per-billion range[32] as required for indoor air quality assessments and other environmental monitoring applications. Use of an integrated array of SAW sensors will provide response patterns which, when coupled with chromatographic retention times, should yield enhanced identification of resolved and coeluting analytes. Results of instrument performance tests will be reported subsequently.

ACKNOWLEDGMENT

The authors express their appreciation to the following individuals: Ms. Tincuta Veriotti of the University of Michigan; Dr. Gregory Frye-Mason, Dr. Patrick Lewis, and Dr. Richard Kottenstette of Sandia National Laboratories; and Dr. Jay Grate of Pacific Northwest National Laboratories. Funding for this work was provided by Grant R01-OH03692 from the National Institute for Occupational Safety and Health of the Centers for Disease Control and Prevention (NIOSH-CDCP). Additional support provided by the University of Michigan Center for Wireless Integrated Microsystems (WIMS) through the Engineering Research Centers Program of the National Science Foundation under Award EEC-9986866 is also gratefully acknowledged.

Received for review April 2, 2001. Accepted July 25, 2001.

AC0103726